

# Biological Implications of the Ribosome's Stunning Stereochemistry

Ella Zimmerman and Ada Yonath\*<sup>[a]</sup>

[a] Dr. E. Zimmerman, Prof. A. Yonath  
Department of Structural Biology  
Weizmann Institute of Science  
76100 Rehovot (Israel)  
Fax: (+972) 8934-4154-4136  
E-mail: ada.yonath@weizmann.ac.il

**THIS COPY WAS CREATED BY THE  
AUTHORS**

DOI: 10.1002/cbic.200800554

# Biological Implications of the Ribosome's Stunning Stereochemistry

Ella Zimmerman and Ada Yonath\*<sup>[a]</sup>

*The ribosome's striking architecture is ingeniously designed for its efficient polymerase activity in the biosynthesis of proteins, which is a prerequisite for cell vitality. This elaborate architecture is comprised of a universal symmetrical region that connects all of the ribosomal functional centers involved in protein biosynthesis. Assisted by the mobility of selected ribosomal nucleotides, the symmetrical region provides the structural tools that are required not only for peptide bond formation, but also for fast and*

*smooth successive elongation of nascent proteins. It confines the path along which the A-tRNA 3'-end is rotated into the P-site in concert with the overall tRNA/mRNA sideways movement, thus providing the required stereochemistry for peptide bond formation and substrate-mediated catalysis. The extreme flexibility of the nucleotides that facilitate peptide bond formation is being exploited to promote antibiotic selectivity and synergism, as well as to combat antibiotic resistance.*

## Introduction

Gene expression requires machinery for the translation of linear DNA sequences into the corresponding linear sequences of amino acids that will eventually become proteins. The complex apparatus responsible for this process is comprised of over 100 cellular components, among them RNA-rich particles, associated with the endoplasmic reticulum, that were detected in the middle of the 20th century and have been suggested to provide sites for gene expression.<sup>[1,2]</sup> These particles, which were initially called "Palade Particles" and later "ribosomes," are the main players of this process. They act as the largest known macromolecular enzymes and provide the machinery for this process. Constant programmed cell death (corresponding with constant protein degradation) requires the simultaneous production of proteins. Hundreds of thousands of ribosomes are present in typical mammalian cells. Quickly replicating cells, for example hepatocytes, can contain a few million ribosomes, even bacterial cells can contain up to 100 000 ribosomes during their logarithmic growth period.

Ribosomes act as polymerases that synthesize proteins by adding one amino acid at a time to a growing peptide chain, while translocating along the messenger RNA (mRNA) template. They produce nascent proteins on a continuous basis at an incredible speed of about 20 peptide bonds per second, and the entire process is highly regulated by various translation factors. Intensive biochemical research over the last half century has resulted in a fairly detailed description of various ribosomal functions, as well as in the physicochemical characterization of the ribosome's numerous components. These studies showed that in all species ribosomes are built of two unequal subunits that associate to perform protein biosynthesis. Each subunit is a giant assembly of long chains of ribosomal RNA (rRNA), in which many ribosomal proteins (r-proteins) are entangled. The ratio of rRNA to r-proteins (~2:1) is maintained throughout evolution, with the exception of mammalian mitochondrial ribosome, in which almost half of the bacteri-

al rRNA is replaced by r-proteins. Within the assembled functional ribosome (Figure 1 A), the small subunit provides the path along which the mRNA progresses, the decoding center, and the mechanism that controls translation fidelity. The large subunit contains the catalytic site, where the polymerization of amino acids occurs, and the protein exit tunnel, along which nascent proteins progress until they emerge out of the ribosome.

The tRNA molecules that carry the amino acids to be incorporated into the growing nascent chains are double-helical, L-shaped molecules that contain an anticodon loop, which matches its complementary three-nucleotide codes on the mRNA, and a 3'-end, which is a single strand with the universal sequence CCA, to which the cognate amino acid is bound covalently. The tRNA molecules are the non-ribosomal entities that combine the two subunits as their three binding sites, A- (aminoacyl), P- (peptidyl), and E- (exit) sites, reside on both subunits of the ribosome. At the A- and P-sites, the tRNA anticodon loops interact with the mRNA on the small subunit, and their acceptor stems with the aminoacylated or peptidylated 3'-end are located on the large subunit.

Efforts initiated at the beginning of the 1980s<sup>[3]</sup> and followed by two decades of progressive methodical developments,<sup>[4]</sup> yielded high-resolution three-dimensional structures of ribosomal particles and their complexes with substrate analogues, inhibitors, antibiotics, and non-ribosomal factors, which facilitate the translation process and initial nascent protein folding. These structures revealed that the ribosome's architecture and its inherent mobility provide the machinery for all stages of

[a] Dr. E. Zimmerman, Prof. A. Yonath  
Department of Structural Biology  
Weizmann Institute of Science  
76100 Rehovot (Israel)  
Fax: (+972)8934-4154-4136  
E-mail: ada.yonath@weizmann.ac.il

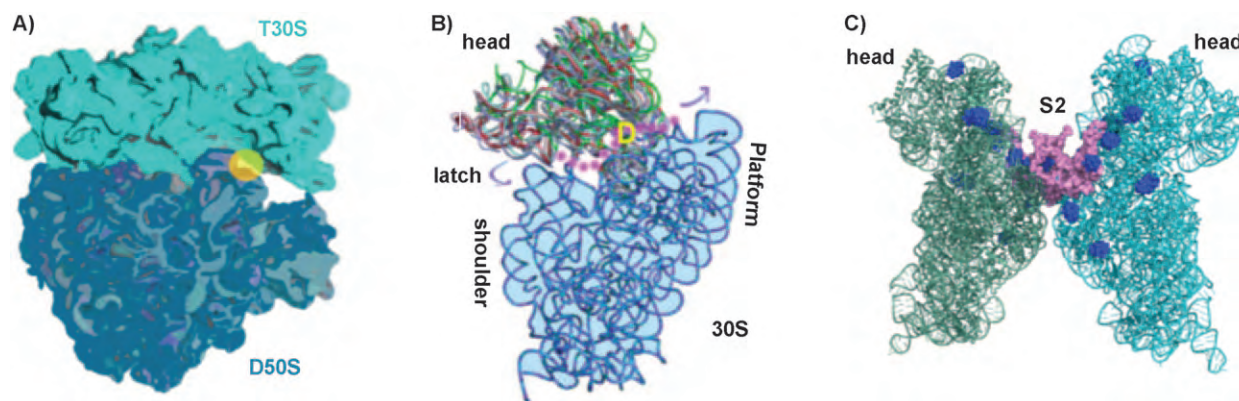


**Figure 1.** Functional mobility of the small subunit. A) The assembled 70S ribosome (obtained by docking the two ribosomal subunits, T30S<sup>[8]</sup> and D50S<sup>[11]</sup> based on the available structures of the entire ribosome<sup>[8,12,13]</sup>); the approximate position of the decoding center (the yellow circle) is indicated. B) Superposition of all known structures of the small ribosomal subunit, showing the “front view” (namely, the intersubunit interface), represented as its rRNA backbone. (Blue: T30S<sup>[8]</sup>; pink and beige: two traceable folds among the ensemble of conformations that exist in T30S low resolution crystals;<sup>[8]</sup> cyan and green: the two conformations that exist in the crystal structure of the entire ribosome from *E. coli*, E70S;<sup>[9]</sup> grey and purple: the conformation within the functional complexes of the entire ribosome from *T. thermophilus*, T70S<sup>[12,13]</sup>) The figure shows the main architectural features (head, platform, shoulder, and latch), the approximate positions of the mRNA channel (pink dots) and of the decoding center (D) and various folds of the “head” that indicate its functional flexibility. It also hints at the feature that is supposed to enable the head mobility—the slender connection between it and the rest of the subunit. The directions of two functional motions are indicated by arrows. The left arrow represents the latch-closing motion that creates a pore for the incoming mRNA. The right arrow represents the coordinated platform–head motion. Together, these motions facilitate mRNA attachment and progression. Because the structure of the body is almost identical in all known crystal structures, only that of T30S<sup>[8]</sup> is shown (blue ribbons and cyan filling). C) Head mobility and its fixation by the heteropolytungstate clusters. Most of the heteropolytungstate cluster molecules bound to T30S<sup>[8]</sup> are shown as blue balls. R-protein S2 of the two adjacent particles (shown in purple) intertwine and provide the forces that stabilize the “head” conformation.

protein biosynthesis and enable its active involvement in the process (reviewed in ref. [5]). Comparative analysis of these structures, and their integration with structural observations obtained by other methods, such as cryo-electron microscopy (EM) and single-molecule fluorescence spectroscopy, confirmed that while elongation proceeds, the two subunits perform cooperatively, and all of the functional tasks that comprise translation are performed mainly, albeit not exclusively, by ribosomal RNA. This analysis also showed that the ribosome is a dynamic molecular machine that utilizes conformational rearrangements as an integral part of the translation machinery. Interpolations between crystal structures that represent the various functional states enabled the dynamic description of several key components of ribosomal function.

This article focuses on the biological implications of the crystallographic findings, with an emphasis on the chemical aspects of the translation process. It highlights the link between ribosomal architecture, its significant conformational mobility, and the reactions that it catalyzes, including successive peptide bond formation and tRNA release. It also addresses issues such as chirality discrimination, the universality of the tRNA CCA end, and the possible chaperone activity of the ribosome. It also shed light on the chemical characterization of the action of ribosomal antibiotics, their selectivity, synergism, and mechanisms for acquiring resistance to antibiotics. These target ribosomes because of their key contribution to a fundamental life process.

## Initiation and Decoding: Architectural Considerations

The initiation of protein biosynthesis is an incredibly intricate process.<sup>[6]</sup> This dynamic step is triggered by initiation factors and the construction of the initiation complex, which is composed of the small ribosomal subunit, mRNA, and an initiator tRNA. It hinges on the accurate positioning of mRNA on the small ribosomal subunit, which is a prerequisite for correct translation. As is the case for all other main ribosomal tasks, mRNA positioning is guided and controlled by the elaborate ribosomal architecture, which contains a purine-rich sequence made of a few nucleotides, called the “Shine–Dalgarno sequence” in prokaryotes. This sticky sequence anchors the 5′-end of the mRNA onto the small ribosomal subunit through the formation of numerous interactions, including base pairing.<sup>[7]</sup>

mRNA binding involves a latch-like closing–opening mechanism<sup>[8–9]</sup> that is performed by the small subunit by coordinated “head”–“shoulder” and “head”–“platform” motions (Figure 1 B). These movements can be minimized either naturally, through the entrance of mRNA into its groove on the small subunit, or chemically, by post crystallization chemical treatment with minute amounts of the heteropolytungstate  $[(\text{NH}_4)_6(\text{P}_2\text{W}_{18}\text{O}_{62}) \cdot 14\text{H}_2\text{O}]$ . This tungstate cluster played a dual role in the determination of the structure of the small ribosomal subunit. In addition to providing anomalous phasing power, it dramatically increased the resolution of the X-ray diffraction from the initial 7–9 Å to 3 Å. Further analysis showed that the tungstate clus-

ter was securely and quantitatively attached to well-defined locations of the small subunit, thus stabilizing a selected functional conformation (the "open latch") within crystals containing more than two different head conformations (Figure 1B). Fourteen cluster molecules bind to each of the crystallized small ribosomal subunits through interactions with positively charged side chains of the extended loops or with the termini of r-proteins exposed on the ribosome surface. Among those, four are attached to the r-protein S2, which possesses extremely flexible, long, and positively charged C and N termini (Figure 1C), in a manner that consequently influences the rigidity of the subunit by controlling the internal flexibility of the region surrounding the mRNA chain, and by gluing together proximal pairs of crystallized particles.<sup>[10]</sup>

Once the initiator tRNA binds to the start codon (AUG) at the P-site, which is downstream of the sticky sequence that anchors and direct the mRNA binding, the construction of the initiation complex is completed. The two subunits associate, and intersubunit bridges are formed by conformational rearrangements.<sup>[11–14]</sup> Local ribosome mobility also plays a major role in the selection of the incoming aminoacylated tRNAs (aa-tRNAs) and in proofreading translation;<sup>[15–17]</sup> the inherent flexibility of the decoding center for monitoring base pairing at the first two positions of each codon is exploited. Noncanonical base pairs at the third position are tolerated by the ribosome.

Among the newly formed intersubunit bridges, B1a (the A-finger; Figure 2A and B) and B2a (the connecting element between the peptidyl-transferase-center (PTC) environs in the large subunit with the decoding center in the small subunit) play key roles in substrate accommodation and positioning. Located at the heart of the ribosome, B2a (helix H69 of the large subunit) is a highly flexible, multifunctional feature. In the assembled ribosome, regardless of its source (*Thermus thermophilus* or *E. coli*, T70S and E70S, respectively) and/or its functional state, B2a stretches out towards the small subunit and interacts with both the A-site and the P-site tRNA molecules.<sup>[9,12–14]</sup> However, in the unbound large subunit of *Deinococcus radiodurans*, D50S, it is positioned at the subunit interface with a distinctly different conformation.<sup>[11]</sup> The significant flexibility of the bridges that allow their conformational rearrangements also seems to facilitate the deactivation of ribosomes under unfavorable conditions. Thus, these bridges can become readily disordered under conditions that are far from physiological, as was observed in crystal structures of the large ribosomal subunit from *Haloarcula marismortui*, H50S.<sup>[18]</sup>

The motions of bridge B1a, which appears to also act as a guide for the entrance of A-site tRNA, are limited by a particular r-protein called L25, TL5, and CTC in *E. coli*, *T. thermophilus* and *D. radiodurans*, respectively. This protein seems to have evolved according to environmental conditions. In the mesophile *E. coli*, the single domain ribosomal protein (r-protein) L25 is located on the solvent side of this bridge in a position that prevents slippage of this bridge away from the core particle. In the thermophile *T. thermophilus*, one of the two domains of r-protein TL5 is replaced by L25, and its second domain interacts with B1a from its other solvent side so that the two domains can hinder almost all uncontrolled motions of this

bridge towards the ribosome periphery; this provides additional stability at high temperature. In *D. radiodurans*, which is a remarkably robust organism that can survive under extreme stress conditions including starvation, irradiation, and in high as well as low temperatures, this protein (called CTC, after a general shock protein) replaces the *E. coli* r-proteins L25 and its homologue TL5 in T50S (Figures 2A and B). Within the known members of the CTC protein family, the CTC protein from *D. radiodurans* is the longest. It contains 253 residues, which makes it about 150 residues longer than L25 and 60 residues longer than TL5. CTC contains three domains. The third domain can reach the A-site and restrict the space that is available for the tRNA molecules. Because it is built of three long  $\alpha$  helices connected by a pointed slim end that can function as a flexible hinge, CTC can control or even eliminate A-site tRNA binding under unfavorable conditions. Hence, it might be part of the mechanisms that *D. radiodurans* developed for survival under extremely stressful conditions.<sup>[19]</sup>

In prokaryotes, three non-ribosomal protein factors are involved in initiation. Initiation factor 3 (IF3) binds to the small subunit in proximity to the mRNA-progressing channel, and its C-terminal domain interacts extensively with the flexible termini of r-protein S18, which protrudes into the solution. Interestingly, one of the heteropolytungstate molecules that binds to the small subunit stabilizes the conformation of the flexible termini of r-protein S18, mimics the conformation required for binding of the C-terminal domain of initiation factor IF3, and competes with its binding.<sup>[20–21]</sup> In this position the C-terminal domain of IF3 can interfere with subunit association and promote the fidelity of P-site codon–anticodon interactions by exploiting its inherent flexibility for positioning of its N terminus domain. Once the initial P-site tRNA binds, the two subunits associate to form the functional ribosome concomitantly with IF3 dissociation.<sup>[22]</sup> In eukaryotes, more regulatory factors are involved; this increases the complexity of this step by an order of magnitude.<sup>[23]</sup>

## Is Substrate Positioning always Apt for Peptide Bond Formation?

Progression of the mRNA by one codon at a time along its defined path from the A- to the P-site in the 3'-to-5' direction is guided by the ribosome's architecture, which provides the geometrical means for preventing backwards or sideways slippage of the mRNA, namely a kink in the mRNA path that separates the A-site from the P-site in the decoding center.<sup>[7–8,12–14]</sup> Large-scale lateral movements of two large subunit stalks, which are called L7/L12 and L1 (Figure 2A) assist A-site tRNA entrance and E-site tRNA exit, respectively.<sup>[5,11,14,19]</sup> A-to-P-site passage of the mRNA and the two tRNAs that are bound to it that occurs in each elongation cycle is driven by the GTPase activity of two elongation factors Tu (EF-Tu) and G (EF-G). The peptide bond is formed in the large subunit simultaneously with the advancement of the mRNA/tRNA along the mRNA path in the small subunit. This process involves the translocation of the tRNA 3'-end from the A- to the P-site within the PTC concurrently with mRNA progression, detachment of the



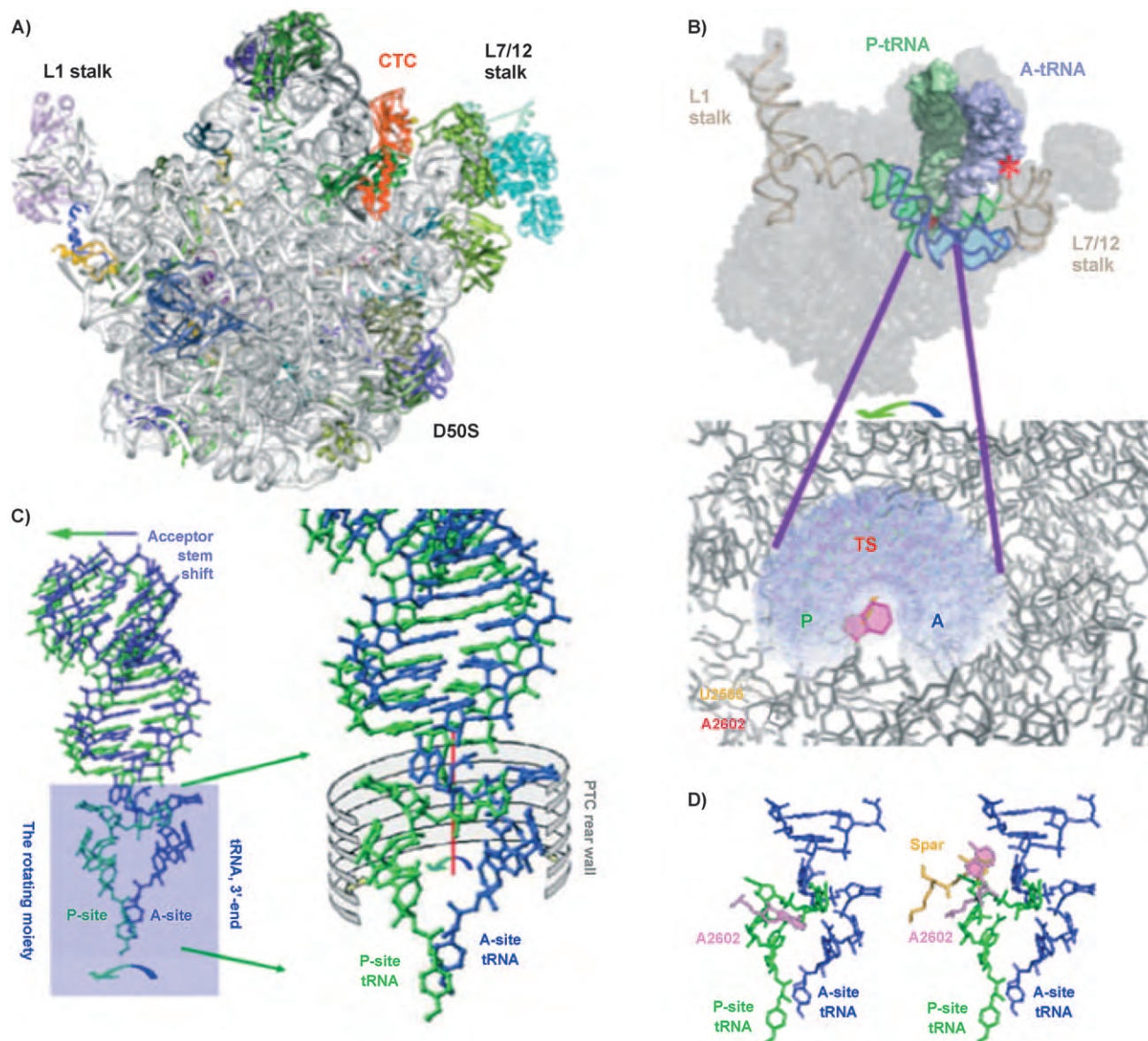


**Figure 2.** Architectural elements that facilitate peptide bond formation and nascent chain elongation. The A-site tRNA (or its mimic) and the derived P-site tRNA are shown in blue and green, respectively. A) The interface face of the large subunit, D50S,<sup>[11]</sup> is shown as ribbons. The rRNA is grey, except for bridge B1a (the A-finger), which is shown in yellow. The r-proteins are blue, green, and purple, except for CTC, which is shown in orange. The mobile structural features that participate in the translation process (L1 and L7/12 stalks) are marked. B) Top: The location of the symmetrical region and its extensions within the large subunit, indicating its central role in connecting all of the ribosomal functional regions that are involved in amino acid polymerization, including L7/L12, which acts as the A-site tRNA entrance site, and L1, which serves as the E-tRNA exiting gate, both known to undergo a coordinated lateral movements during elongation. Bridge B2a extends towards the decoding center in the small subunit (not shown). The two symmetrical subregions that contain the A- and the P-sites are shown in blue and green, respectively, and the extensions, which comprise the L1 and L7/12 stalks are shown in gold. The red “snowflake” indicates the position of protein CTC and of bridge B1a that is adjacent to it. Bottom: The PTC region is enlarged. The ribosomal RNA is shown in grey, except for the two anchoring–propelling nucleotides, A2602 and U2585, which are shown in magenta and orange, respectively. The void that is available for the tRNA 3′-end translocation is in light blue (constructed by simulation of the rotatory motion). The approximate positions of the A and the P-sites as well as of the quantum-mechanical-computed transition state of this reaction (TS) are indicated. C) The tRNA-synchronized motions are comprised of a sideways shift, which is performed as a part of the overall mRNA/tRNA translocation, and the rotatory motion of the A-tRNA 3′-end along a path confined by the PTC walls. The rRNA nucleotide comprises the PTC walls that confine the rotatory motion are shown in grey. The directions of the two components of the tRNA motions are indicated by blue-green arrows, and the imaginary twofold symmetry axis is in red. D) The flexibility of nucleotide A2602. Two conformations of this nucleotide, rotated 180° apart, as obtained in native D50S<sup>[11]</sup> and in its complex with sparsomycin<sup>[33]</sup> (called: SPAR). A-site tRNA mimic (ASM in ref. [8]) and the derived P-site tRNA are shown in blue and green, for orientation.

P-site tRNA from the growing polypeptide chain, passage of the deacylated tRNA molecule into the E-site and subsequent release of the tRNA molecule.

At the early stages of ribosome research, ribosomal proteins were believed to perform most ribosomal functional tasks, including the catalysis of peptide bond formation. At that time

ribosomal RNA was thought to provide the scaffold that holds the numerous ribosomal proteins in an orientation that allows them to perform their tasks.<sup>[24,25]</sup> In the late 1980s the importance of ribosomal RNA (rRNA) became evident,<sup>[26]</sup> and in the 1990s the dominance of rRNA in ribosome functional activity was proven biochemically.<sup>[27]</sup> All available crystal structures<sup>[9,11–14,18]</sup> show that in the assembled bacterial ribosomes, the intersubunit interface surfaces are rich in rRNA. Because both the decoding center and the site of peptide bond formation (called the PTC) reside in proximity to the intersubunit interface, they are located in rRNA-predominant environments. Based on the high sequence conservation of the interfacing ribosomal regions, it is conceivable that the intersubunit interfaces of all ribosomes throughout evolution, are rich in rRNA. Hence, unlike typical polymerases, which are pure protein enzymes, the major, albeit not the only, player in the polymerase activity of the ribosome is rRNA. Thus, although a single peptide bond can be formed in a protein-free environment, a few proteins (L2, L16, L27) seem to assist the subsequent steps like the sequential repetition of this reaction, or, in other words, amino acids polymerization (reviewed in refs. [10], [19] and [28]).

Despite the extensive studies aimed at the identification of the chemical nature of the initial step in protein biosynthesis (namely the creation of the first peptide bond), the fine details of this step and the precise contribution of the ribosome to it have remained controversial, and are still not fully characterized (reviewed in ref. [29]). The initial suggestion that three specific rRNA nucleotides catalyze peptide bond formation by the general acid–base mechanism that was based on the crystal structure of complexes of the large ribosomal subunit from *Haloarcula marismortui* (H50S), which was determined under far from optimal functional conditions,<sup>[18]</sup> was quickly challenged by a battery of biochemical and mutational studies.<sup>[30–32]</sup>

It appears that the choice of substrate analogues is partially responsible for the misinterpretations. Thus, although aminoacylated tRNA molecules are the natural substrates of ribosomes, “minimal substrates”, which are also called “fragment reaction substrates” and are capable of producing only a single peptide bond, are commonly used biochemically. Typical “minimal substrates” are derivatives of puromycin (*O*-methyl tyrosine that is linked to N6-dimethyl adenosine through an amide bond). They resemble the tip of the aminoacylated-tRNA CCA end, but lack the hydrolysable ester function. Their small size leads one to the assumption that such substrates can readily diffuse into the PTC in a more efficient fashion than full-length tRNA molecules. However, biochemical and kinetic studies indicate that the peptide bond formation by “minimal substrates” is significantly slower than that of full-length aminoacylated-tRNAs. This unpredictable finding was one of the intriguing issues to which no suitable explanation was available before the crystal structures of ribosomes in complex with various substrate analogues were determined.

Architectural elements that contribute to peptide bond formation were identified in the structures of a complex of D50S with different-sized constructs that mimic specific parts of aminoacylated tRNA. One of those is an analogue of the tRNA ac-

ceptor stem and its aminoacylated 3'-end (ASM), which is the entire fraction of A-site tRNA that binds to the large subunit. The other structure is a minimal substrate that mimics the aminoacylated tRNA CCA end.<sup>[33–34]</sup> Although both complexes were obtained under the same conditions, which were optimized for efficient protein biosynthesis, these two substrate analogues bind to the PTC in different orientations. Thus, ASM, which resembles a full-length tRNA, is aligned by an extensive net of interactions between its acceptor stem and the cavity that leads to the PTC.<sup>[33]</sup> These interactions govern its accurate positioning in the PTC at the precise orientation that is required for efficient and smooth peptide bond formation. In contrast, only a few interactions are created by the “minimal substrate.” These few interactions enable the minimal substrate to utilize the space of the A-site tRNA 3'-end, but at a slightly different orientation; similar to those obtained for H50S complexes with various minimal substrates, most of which require additional positional rearrangements to reach the precise orientation that is required for peptide bond formation.<sup>[35,36]</sup> Thus, the D50S–ASM complex demonstrates the significance of the interactions between the tRNA acceptor stem and the walls of the cavity that leads to the PTC. Comparisons between the positioning of ASM and the “minimal substrates” in complexes with D50S as well as with H50S shed light on the PTC's ability to accommodate substrates at approximate orientations.<sup>[36]</sup> Consistently, the overwhelming differences in the duration of the formation of single peptide bonds by “minimal substrates” and by full-length tRNAs are rationalized by the requirement of the latter to undergo positional rearrangements due to their approximate positioning.<sup>[35,36]</sup>

Incorporating structural data that was obtained from additional ribosomal crystal forms highlights the PTC's remarkable ability to rearrange itself upon substrate binding<sup>[12,36]</sup> and verifies the findings that the peptidyl transfer reaction is modulated by conformational changes at the active site.<sup>[37–40]</sup> Notably, the D50S–ASM complex<sup>[33]</sup> is so far the only complex with an A-site tRNA mimic that extends beyond the tip of the tRNA 3'-end, although crystals supposedly containing assembled ribosomes with two and/or three tRNA molecules have been subjected to crystallographic analysis.<sup>[12–13]</sup> The current conclusions, which are based on comparing the structures of ribosomes with substrate analogues of various lengths, advanced the comprehension of peptide bond formation significantly. They indicate that rather than participating chemically in peptide bond formation, the ribosomal architecture positions its natural substrates in an orientation that is suitable for peptide bond formation, thus providing positional catalysis.<sup>[33–34]</sup> Importantly, peptide bonds can be formed in a semiefficient manner by compounds that possess various conformations, some of which mimic approximately parts of the tRNA substrates,<sup>[18,27,35,37,41]</sup> and hence require ribosomal and/or substrate rearrangements for proper substrate positioning<sup>[5,34]</sup> and for promoting substrate-mediated chemical acceleration of peptide bond formation.<sup>[40–42]</sup> This is in accord with the finding that rapid and smooth peptide bond formation requires full-length tRNA in both the A and P sites, as observed by chemi-

cal,<sup>[40,42–43]</sup> atomic,<sup>[44]</sup> and molecular mutagenesis,<sup>[45,46]</sup> computational,<sup>[47–49]</sup> and kinetic<sup>[38,39,50,51]</sup> methods.

The currently accepted view of the mechanism of peptide bond formation is consistent with ribosomal positional catalysis that is accelerated and assisted by its P-site tRNA substrate. However, despite intensive efforts to elucidate the details of peptide bond formation by various noncrystallographic methods (review in ref. [52]) the detailed mechanism of peptide bond formation is still a mystery, and may be revealed by X-ray structures of ribosomes that contain both the aminoacylated and the peptidyl tRNAs in the PTC.

## From Peptide Bond Formation to Amino Acid Polymerization

If time is not an issue, single peptide bonds can be formed with no assistance whatsoever, but the repetition of this reaction requires elaborate architecture. As the ribosome's main task is amino acid polymerization; it provides the means not only for the mere formation of peptide bonds, but also for the progression of the reaction.

Both peptide bond formation and the ribosomal polymerase activity are governed by the striking architecture of the ribosome. Although the ribosome is asymmetric, it contains a highly conserved region of 180 nucleotides (Figure 2B), in which the rRNA fold and the orientations of its nucleotides, but not their sequences, are related by pseudo twofold symmetry.<sup>[33–34]</sup> This sizable intraribosomal symmetrical region has been identified in all known structures of large ribosomal subunits, regardless of their source (mesophilic, thermophilic, radiophilic, and halophilic bacteria), their kingdom of life (eubacteria and archaea), their functional state (assembled ribosome or unbound subunit, and their complexes with substrate analogues or inhibitors). Remarkably, despite the significant size differences between ribosomes from various kingdoms of life, the functional regions of the ribosomes are rather well conserved, with the highest level of sequence conservation at their central core, and the largest structural differences located at the periphery. The core contains the symmetrical region in which 98% of the nucleotides are found in >95% of sequences (from 930 different species from the three domains of life), but, remarkably, only 36% of all *E. coli* nucleotides, excluding the symmetrical region, can be categorized as such. Importantly, 75% of the 27 nucleotides that lie within 10 Å of the symmetry axis are highly conserved. Among them, seven are completely conserved.<sup>[34]</sup>

The universality of the symmetrical region and the high level of sequence conservation that was detected even in mitochondrial ribosomes, in which half the ribosomal RNA is replaced by proteins, and the ability of this region to provide all of the structural elements required for performing polypeptide elongation, suggest that the ribosome evolved by gene fusion or duplication. Furthermore, the preservation of the three-dimensional structure of the two halves of the ribosomal frame, regardless of the sequence, demonstrates the rigorous stereochemical requirements for accurate substrate positioning during peptide bond formation. This, as well as the universality

of the symmetrical region, led to the assumption that the ancient ribosome contained a similar pocket that was confined by two RNA chains.

The symmetrical region is located in and around the PTC, and connects, either directly or by its extensions, all ribosomal functional regions that are involved in amino acid polymerization, including the tRNA entrance/exit dynamic stalks, the PTC, and the bridge that connects the PTC cavity with the vicinity of the decoding center in the small subunit and the nascent protein exit tunnel (Figure 2B). Hence, it can serve as the central feature for signaling between all the functional regions that are involved in protein biosynthesis, that are located remotely from each other (up to 200 Å away), but must "talk" to each other during elongation,<sup>[34]</sup> thus guaranteeing smooth succession of amino acid polymerization. A suitable example is the direct connection between peptide bond formation in the large subunit and the association of the mRNA with the small subunit.<sup>[53]</sup>

The linkage between the elaborate PTC architecture and the A-site tRNA position that was observed crystallographically<sup>[33]</sup> indicates that the translocation of the tRNA 3'-end is performed by a combination of two independent, albeit synchronized motions: a sideways shift, which is performed as part of the overall mRNA/tRNA translocation, and a rotatory motion of the A-tRNA 3'-end, around the bond connecting it with the tRNA helical regions along a path that is confined by the PTC walls (Figures 2B and C). This bond coincides with an imaginary axis that passes through the symmetry-related region. The rotatory motion is guided by a rRNA scaffold along an exact pattern (called the PTC "rear wall") and results in stereochemistry that is optimal for peptide bond formation, and in a geometry that ensures the entrance of nascent proteins into their exit tunnel. While the PTC rear wall confines and guides the rotatory path, two universal nucleotides A2602 and U2585 (*E. coli* nomenclature throughout) of the PTC "front wall", which bulges towards the twofold symmetry axis and do not obey the twofold symmetry, anchor this motion. Both nucleotides are highly flexible (Figure 2D), and their mobility appears to play major roles in the rotatory motion. The nucleotide A2602 seems to propel the motion, and potential rearrangements of U2585 seem to facilitate chirality discrimination and ensure proper chirality by prohibiting D-amino acid incorporation.<sup>[54]</sup>

The rotatory motion positions the proximal 2'-hydroxyl of the P-site tRNA A76 in the same position and orientation that is found in crystals of the entire ribosome with mRNA,<sup>[12–13]</sup> and allows for chemical catalysis of peptide bond formation by A76 of the P-site tRNA.<sup>[42]</sup> It therefore appears that the ribosomal architecture and its mobility provides all of the structural elements that enable the ribosome to function as an amino acid polymerase, including the formation of two symmetrical universal base pairs between the tRNAs and the PTC,<sup>[33–34]</sup> thus allowing for a prerequisite for substrate-mediated acceleration<sup>[42]</sup> and for the direction of the nascent protein into the exit tunnel.

Simulation studies indicated that during the rotatory motion, the rotating moiety interacts with ribosomal nucleotides and confines the rotatory path along the PTC "rear



wall."<sup>[34]</sup> Some of those interactions are made with the bases of these nucleotides. Other contact exploits the rRNA backbone, and thus, despite the key contributions of these nucleotides to smooth translocation and efficient amino acid polymerization, their bases can be mutated, as found by comprehensive mutagenesis.<sup>[46]</sup> Consistently, quantum mechanical calculations based on the D50S structural data and the quantification of the interactions between the rotating moiety indicated that the transition state (TS) is being formed during the rotatory motion and is stabilized by hydrogen bonds with rRNA nucleotides of the PTC "rear wall".<sup>[49]</sup>

This mode of operation allows the aminoacylated tRNA to move into the P-site, while the deacylated former P-site tRNA moves toward the E-site. Simultaneously, the PTC A-site is gradually evacuated by its former occupant, and hence can host the next substrate, which approaches as a result of the global mRNA/tRNA progression along its path in the small subunit. Importantly, the transition state (TS) found by quantum mechanical computations is within the space available between the A and the P-sites, but closer to the latter (Figure 2B). This TS position and orientation are similar to the one found experimentally in the crystal structure of a complex of the large subunit from a ribosome from a different source, H50S, with a transition state analogue that was designed chemically.<sup>[37]</sup> The correlation between the rotatory motion and amino acid polymerization rationalize the apparent contradiction that is associated with the location of the growing protein chain. Thus, traditional biochemical methods for the detection of ribosomal activity were based on the reaction between substrate analogues, which were designed for producing a single peptide bond, and do not involve an A-to-P-site translocation. However, elongation requires substrates that are suitable to perform the A-to-P-site passage and the entrance to the ribosome tunnel, near the location of the properly designed TS analogues<sup>[37]</sup> as well as the calculated TS position.<sup>[49]</sup>

### Mobility and Remote Networks Facilitate Antibiotics Selectivity

As it is a key player in cell vitality, the ribosome is targeted by many useful antibiotics. These hamper protein synthesis in bacterial pathogens by diverse mechanisms (for review see refs. [5], [20], [55] and [56]). Because no crystal structures of ribosomes from genuine pathogens are available yet, the structures of ribosomes from *D. radiodurans* and *T. thermophilus*, two eubacteria that have been proven to serve as suitable pathogen models, have been investigated in complex with various antibiotics. These show that among the modes of action of ribosomal antibiotics, the antibiotics cause miscoding, minimize essential mobility, interfere with substrate binding at the decoding center and at the PTC, and block the protein exit tunnel. Binding sites that are composed primarily of rRNA and coincide with functional centers of the ribosome are common to ribosomal antibiotics.

Although prokaryotic and eukaryotic ribosomes differ in size (~2.4 and 4 MDa, respectively), they are highly conserved functionally. Therefore the imperative distinction between eubacte-

rial pathogens and eukaryotes, the key for antibiotics usefulness, is achieved mainly, albeit not exclusively, by subtle structural differences within the antibiotic's binding pockets. A striking example for subtle discrimination between eubacteria and higher organisms is the minute difference between adenine and guanine in position 2058, which was found to govern the binding of macrolides. The macrolides are a prominent family of antibiotics that obstruct the progression of the nascent proteins along their tunnel.<sup>[57]</sup> As this tunnel plays a multifunctional role, tunnel blocking might have more consequences than the mere blockage of nascent proteins' progression. The tunnel provides co-translational protection to newly born proteins, its dynamic properties facilitate its involvement in the nascent chain's sequence-specific gating, and may possess chaperoning properties at a crevice for transient cotranslational folding (review in ref. [5]). Comparisons of crystal structures of the eubacterial large ribosomal subunit, D50S,<sup>[56-57]</sup> and large subunits of the archaeon that share properties with eukaryotes, H50S, as well as of a H50S mutant, G2058A,<sup>[60]</sup> verified that the nucleotide at position 2058 is responsible for macrolide binding. These structures also showed, however, that mere binding is not sufficient for clinical effectiveness, and indicated the significance of additional structural elements<sup>[20]</sup> that dictate the level of inhibitory activity; this is consistent with A→G mutagenesis in yeast at a position equivalent to *E. coli* A2058, which do not confer erythromycin susceptibility.<sup>[61]</sup>

The core catalytic center, and especially the PTC, of the ribosome is highly (or completely) conserved, the mechanisms for acquiring selectivity are rather complex. Nevertheless, several clinically useful antibiotics bind to the PTC of eubacterial ribosomes (Figure 3A) with high affinity and great specificity, without significant effect on the eukaryotic host. Examples are chloramphenicol, clindamycin, pleuromutilins, streptogramins, oxazolidinones,<sup>[20,58,62-68]</sup> as well as potentially useful antibiotics from the lankacidin family.<sup>[69]</sup> Crystal structures showed that although almost all PTC antibiotics act by blocking a part or the entire PTC, they use different binding modes, and consequently, they possess different inhibitory mechanisms. Chloramphenicol hampers the binding of the A-site tRNA, pleuromutilins, linezolid, and streptogramins<sub>A</sub> occupy both the A and P-site tRNAs, and clindamycin interferes with peptide bond formation. Assuming that most PTC antibiotics use similar structural principles for selectivity and resistance, comprehending the factors that allow for selectivity provides powerful tools to understand many of the mechanisms that are exploited for acquiring resistance.

Among the PTC antibiotics, the streptogramins<sub>A</sub> (group A) are of a special interest because they all exhibit rather weak inhibitory effects if used alone, but can become very potent when used together with their mates from the streptogramins<sub>B</sub> (group B), which are also weakly active on their own. Group A compounds (S<sub>A</sub>) are highly modified cyclopeptides with multiple conjugated double bonds, whereas the group B (S<sub>B</sub>) compounds are cyclic hexadepsipeptides that act as low-affinity macrolides. An impressive synergetic effect is demonstrated by synercid®, a two-component drug (dalfoipristin and quinupristin). Crystal structures showed that the synergetic mechanism



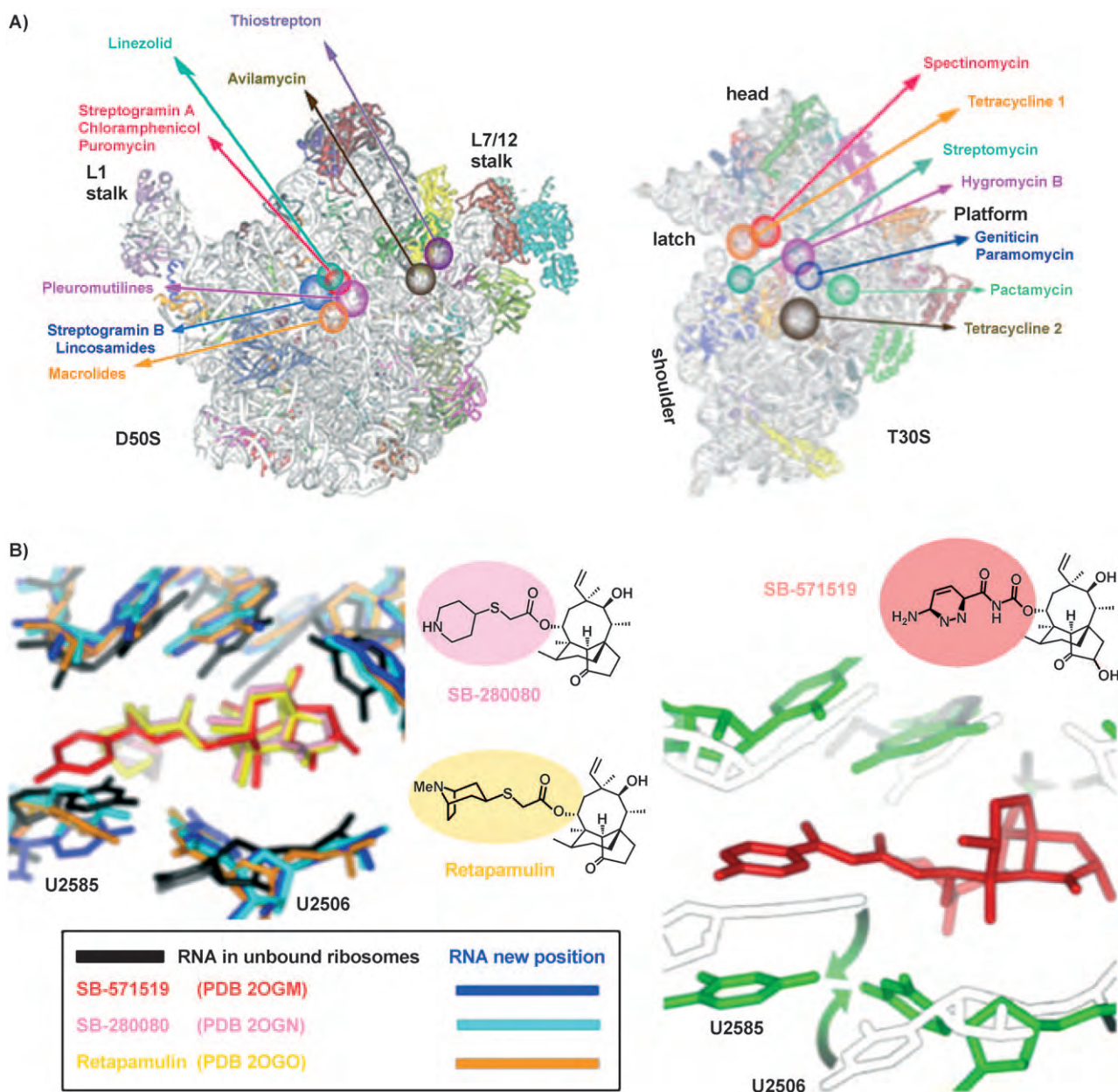


**Figure 3.** Ribosomal antibiotics. A) The positions of most of the ribosomal antibiotics are shown on the interface surfaces of the two ribosomal subunits, T30S<sup>[68]</sup> and D50S,<sup>[111]</sup> which are represented as gray (RNA) and colorful (protein) ribbons. Note that all of the antibiotics are bound to ribosomal functional centers. B) Induced fit and remote interactions of the PTC antibiotics pleuromutilins. All views show only the variable extension (highlighted by the colored balloons). Left: the locations and the induced conformational rearrangements induced by three members of this family are shown. Right: the conformational rearrangements of the rRNA that allow for the accommodation of the drug and creation of the remote interaction network (wild-type rRNA is shown as black frames empty space, and the modified positions are shown in green).

is based on a dramatic alteration in the orientation of the very flexible PTC nucleotide, U2585, which plays a principal role in the A-to-P-site rotatory motion. Thus, the binding of dalfopristin, the  $S_A$  component, to the PTC causes 180° rotation of U2585. This motion seems to be reversible until quinupristin, the  $S_B$  component, is added. This leads to the fixation of U2585 at the altered conformation by hindering its motion as well as by blocking the tunnel entrance and preventing the escape of the  $S_A$  component.<sup>[20,64]</sup>

The contribution of the same flexible nucleotide, U2585, to antibiotics that bind with clinical relevance has been observed

by structural investigation of the mode of action of the pleuromutilin family. This revealed a unique inhibitory mechanism alongside a novel selectivity and resistance strategy. In particular, the elaborate binding mode of the pleuromutilins demonstrates how selectivity and resistance are acquired despite almost full conservation.<sup>[62,67]</sup> Because all nucleotides in the immediate vicinity of the binding site are highly conserved, the selectivity of the pleuromutilins is determined by nucleotides that are located remotely from the antibiotic binding site, hence are less conserved. Thus, pleuromutilins binding triggers an induced-fit mechanism by exploiting the flexibility of the

rRNA nucleotides that reside in and around the PTC, as well as a network of interactions with less-conserved remote nucleotides, hence allowing for drug selectivity.<sup>[67]</sup>

In short, the pleuromutilins exploit the mobility of the extremely flexible nucleotides U2585 and U2506 that participate in navigating and anchoring the rotatory motion. The coordinated motions of these nucleotides evacuate the binding region, and, by triggering additional motions of remote nucleotides they tighten the binding pocket on the bound antibiotic molecule without interacting with it (Figure 3B). This remarkable finding explains the similarity in the inhibitory pattern of members of the pleuromutilin family that have a dramatically different chemical nature, and has opened the way for the design of a large number of new members.<sup>[70]</sup> Furthermore, because most mutations within the PTC should be lethal, resistance to pleuromutilins requires modifications of nucleotides that can be selected from a rather limited pool of less-crucial PTC nucleotides. Alternatively, resistance might be mediated by nucleotides that reside at remote locations from the PTC, but that nevertheless influence its shape by induced fit and/or allosteric mechanisms.<sup>[62,67,71]</sup> Such allosteric motions could be similar to the expected consequences of modification in r-proteins L22 and L4, which cause resistance to macrolides although they do not interact with them.<sup>[72]</sup>

## Conclusions and Future Prospects

Ribosomal crystal structures, in conjunction with numerous biochemical, kinetic and genetic findings, show that the ribosome provides the framework for the proper positioning of the participants of the biosynthetic process and is actively involved in the translation process. Furthermore, the research on ribosomal antibiotics revealed common traits, identified unexpected binding features, led to new insights into ribosomal functional flexibility, and indicated the existence of an allosteric network around the PTC. The value of these findings is far beyond their potential clinical usage, because they highlight basic issues like reshaping of binding pockets by remote networks, and shed light on the fashion that ribosome inhibitors benefit from ribosome functional flexibility. Finally, careful cross-examination of the basic concepts in protein biosynthesis in bacteria showed that they can be connected to properties of higher organisms, like signal transduction and oncogenesis,<sup>[73]</sup> hence the value of these studies opened the path for future studies on protein biosynthesis in the eukaryotic kingdom.

## Acknowledgements

Thanks are due to all members of the ribosome group at the Weizmann Institute for constant interest. Support was provided by the US National Institutes of Health (GM34360), and the Kimmelman Center for Macromolecular Assemblies. A.Y. holds the Martin and Helen Kimmel Professorial Chair.

**Keywords:** antibiotics · peptide bond formation · ribosome · X-ray crystallography

- [1] G. E. Palade, *J. Biophys. Biochem. Cytol.* **1955**, *1*, 59–68.
- [2] J. D. Watson, *Science* **1963**, *140*, 17–26.
- [3] A. Yonath, J. Muessig, B. Tesche, S. Lorenz, V. A. Erdmann, H. G. Wittmann, *Biochem. Int.* **1980**, *1*, 428–435.
- [4] M. Gluehmann, R. Zarivach, A. Bashan, J. Harms, F. Schluenzen, H. Bartels, I. Agmon, G. Rosenblum, M. Pioletti, T. Auerbach, H. Avila, H. A. Hansen, F. Franceschi, A. Yonath, *Methods* **2001**, *25*, 292–302.
- [5] A. Bashan, A. Yonath, *Trends Microbiol.* **2008**, *16*, 326–335.
- [6] A. Marintchev, G. Wagner, *Q. Rev. Biophys.* **2004**, *37*, 197–284.
- [7] G. Yusupova, L. Jenner, B. Rees, D. Moras, M. Yusupov, *Nature* **2006**, *444*, 391–394.
- [8] F. Schluenzen, A. Tocilj, R. Zarivach, J. Harms, M. Gluehmann, D. Janell, A. Bashan, H. Bartels, I. Agmon, F. Franceschi, A. Yonath, *Cell* **2000**, *102*, 615–623.
- [9] B. S. Schuwirth, M. A. Borovinskaya, C. W. Hau, W. Zhang, A. Vila-Sanjurjo, J. M. Holton, J. H. D. Cate, *Science* **2005**, *310*, 827–834.
- [10] A. Bashan, A. Yonath, *J. Mol. Struct.* **2008**, *890*, 289–294.
- [11] J. Harms, F. Schluenzen, R. Zarivach, A. Bashan, S. Gat, I. Agmon, H. Bartels, F. Franceschi, A. Yonath, *Cell* **2001**, *107*, 679–688.
- [12] M. Selmer, C. M. Dunham, F. V. Murphy IV, A. Weixlbaumer, S. Petry, A. C. Kelley, J. R. Weir, V. Ramakrishnan, *Science* **2006**, *313*, 1935–1942.
- [13] A. Korostelev, S. Trakhanov, M. Laurberg, H. F. Noller, *Cell* **2006**, *126*, 1065–1077.
- [14] M. M. Yusupov, G. Z. Yusupova, A. Baucom, K. Lieberman, T. N. Earnest, J. H. Cate, H. F. Noller, *Science* **2001**, *292*, 883–896.
- [15] S. C. Blanchard, R. L. Gonzalez, H. D. Kim, S. Chu, J. D. Puglisi, *Nat. Struct. Mol. Biol.* **2004**, *11*, 1008–1014.
- [16] F. V. Murphy, V. Ramakrishnan, *Nat. Struct. Mol. Biol.* **2004**, *11*, 1251–1252.
- [17] L. Cochella, R. Green, *Nat. Struct. Mol. Biol.* **2004**, *11*, 1160–1162.
- [18] P. Nissen, J. Hansen, N. Ban, P. B. Moore, T. A. Steitz, *Science* **2000**, *289*, 920–930.
- [19] A. Yonath, *Curr. Protein Pept. Sci.* **2002**, *3*, 67–78.
- [20] A. Yonath, A. Bashan, *Annu. Rev. Microbiol.* **2004**, *58*, 233–251.
- [21] M. Pioletti, F. Schluenzen, J. Harms, R. Zarivach, M. Gluehmann, H. Avila, A. Bashan, H. Bartels, T. Auerbach, C. Jacobi, T. Hartsch, A. Yonath, F. Franceschi, *EMBO J.* **2001**, *20*, 1829–1839.
- [22] A. Fabbretti, C. L. Pon, S. P. Hennesly, W. E. Hill, J. S. Lodmell, C. O. Guallerzi, *Mol. Cell* **2007**, *25*, 285–296.
- [23] P. F. Cho, F. Poulin, Y. A. Cho-Park, I. B. Cho-Park, J. D. Chicoine, P. Lasko, N. Sonenberg, *Cell* **2005**, *121*, 411–423.
- [24] R. A. Garrett, H. G. Wittmann, *Adv. Protein Chem.* **1973**, *27*, 277–347.
- [25] R. A. Garrett, H. G. Wittmann, *Endeavour* **1973**, *32*, 8–14.
- [26] H. F. Noller, *Annu. Rev. Biochem.* **1984**, *53*, 119–162.
- [27] H. F. Noller, V. Hoffarth, L. Zimniak, *Science* **1992**, *256*, 1416–1419.
- [28] I. Wekselman, C. Davidovich, I. Agmon, E. Zimmerman, H. Rosenberg, A. Bashan, R. Berisio, A. Yonath, *J. Pept. Sci.* **2008**; in press.
- [29] R. M. Anderson, M. Kwon, S. A. Strobel, *J. Mol. Evol.* **2007**, *64*, 472–483.
- [30] N. Polacek, M. Gaynor, A. Yassin, A. S. Mankin, *Nature* **2001**, *411*, 498–501.
- [31] A. Barta, S. Dorner, N. Polacek, *Science* **2001**, *291*, 203.
- [32] J. Thompson, D. F. Kim, M. O'Connor, K. R. Lieberman, M. A. Bayfield, S. T. Gregory, R. Green, H. F. Noller, A. E. Dahlberg, *Proc. Natl. Acad. Sci. USA* **2001**, *98*, 9002–9007.
- [33] A. Bashan, I. Agmon, R. Zarivach, F. Schluenzen, J. Harms, R. Berisio, H. Bartels, F. Franceschi, T. Auerbach, H. A. S. Hansen, E. Kossoy, M. Kessler, A. Yonath, *Mol. Cell* **2003**, *11*, 91–102.
- [34] I. Agmon, A. Bashan, R. Zarivach, A. Yonath, *Biol. Chem.* **2005**, *386*, 833–844.
- [35] J. L. Hansen, T. M. Schmeing, P. B. Moore, T. A. Steitz, *Proc. Natl. Acad. Sci. USA* **2002**, *99*, 11670–11675.
- [36] A. Yonath, *Biol. Chem.* **2003**, *384*, 1411–1419.
- [37] T. M. Schmeing, K. S. Huang, D. E. Kitchen, S. A. Strobel, T. A. Steitz, *Mol. Cell* **2005**, *20*, 437–448.
- [38] M. Beringer, M. V. Rodnina, *Mol. Cell* **2007**, *26*, 311–321.

- [39] M. Beringer, C. Bruell, L. Xiong, P. Pfister, P. Bieling, V. I. Katunin, A. S. Mankin, E. C. Bottger, M. V. Rodnina, *J. Biol. Chem.* **2005**, *280*, 36065–36072.
- [40] J. L. Brunelle, E. M. Youngman, D. Sharma, R. Green, *RNA* **2006**, *12*, 33–39.
- [41] M. Koch, Y. Huang, M. Sprinzl, *Angew. Chem.* **2008**, *120*, 7352–7355; *Angew. Chem. Int. Ed.* **2008**, *47*, 7242–7245.
- [42] J. S. Weinger, K. M. Parnell, S. Dorner, R. Green, S. A. Strobel, *Nat. Struct. Mol. Biol.* **2004**, *11*, 1101–1106.
- [43] J. S. Weinger, S. A. Strobel, *Biochemistry* **2006**, *45*, 5939–5948.
- [44] K. Lang, M. Erlacher, D. N. Wilson, R. Micura, N. Polacek, *Chem. Biol.* **2008**, *15*, 485–492.
- [45] E. M. Youngman, L. Cochella, J. L. Brunelle, S. He, R. Green, *Cold Spring Harbor Symp. Quant. Biol.* **2006**, *71*, 545–549.
- [46] N. S. Sato, N. Hirabayashi, I. Agmon, A. Yonath, T. Suzuki, *Proc. Natl. Acad. Sci. USA* **2006**, *103*, 15386–15391.
- [47] S. Trobro, J. Aqvist, *Biochemistry* **2006**, *45*, 7049–7056.
- [48] P. K. Sharma, Y. Xiang, M. Kato, A. Warshel, *Biochemistry* **2005**, *44*, 11307–11314.
- [49] A. Gindulyte, A. Bashan, I. Agmon, L. Massa, A. Yonath, J. Karle, *Proc. Natl. Acad. Sci. USA* **2006**, *103*, 13327–13332.
- [50] I. Wohlgemuth, M. Beringer, M. V. Rodnina, *EMBO Rep.* **2006**, *7*, 699–703.
- [51] A. Sievers, M. Beringer, M. V. Rodnina, R. Wolfenden, *Proc. Natl. Acad. Sci. USA* **2004**, *101*, 7897–7901.
- [52] N. Polacek, A. S. Mankin, *Crit. Rev. Biochem. Mol. Biol.* **2005**, *40*, 285–311.
- [53] S. Uemura, M. Dorywalska, T. H. Lee, H. D. Kim, J. D. Puglisi, S. Chu, *Nature* **2007**, *446*, 454–457.
- [54] R. Zarivach, A. Bashan, R. Berisio, J. Harms, T. Auerbach, F. Schlunzen, H. Bartels, D. Baram, E. Pyetan, A. Sittner, M. Amit, H. A. S. Hansen, M. Kessler, C. Liebe, A. Wolff, I. Agmon, A. Yonath, *J. Phys. Org. Chem.* **2004**, *17*, 901–912.
- [55] T. Tenson, A. Mankin, *Mol. Microbiol.* **2006**, *59*, 1664–1677.
- [56] E. C. Bottger, *Trends Biotechnol.* **2006**, *24*, 145–147.
- [57] C. J. Lai, B. Weisblum, *Proc. Natl. Acad. Sci. USA* **1971**, *68*, 856–860.
- [58] F. Schlünzen, R. Zarivach, J. Harms, A. Bashan, A. Tocilj, R. Albrecht, A. Yonath, F. Franceschi, *Nature* **2001**, *413*, 814–821.
- [59] E. Pyetan, D. Baram, T. Auerbach-Nevo, A. Yonath, *Pure Appl. Chem.* **2007**, *79*, 955–968.
- [60] D. Tu, G. Blaha, P. B. Moore, T. A. Steitz, *Cell* **2005**, *121*, 257–270.
- [61] A. S. Bommakanti, L. Lindahl, J. M. Zengel, *RNA* **2008**, *14*, 460–464.
- [62] F. Schlünzen, E. Pyetan, P. Fucini, A. Yonath, J. M. Harms, *Mol. Microbiol.* **2004**, *54*, 1287–1294.
- [63] J. L. Hansen, P. B. Moore, T. A. Steitz, *J. Mol. Biol.* **2003**, *330*, 1061–1075.
- [64] J. M. Harms, F. Schlünzen, P. Fucini, H. Bartels, A. Yonath, *BMC Biol.* **2004**, *2*, 1–10.
- [65] T. Auerbach, A. Bashan, A. Yonath, *Trends Biotechnol.* **2004**, *22*, 570–576.
- [66] A. Yonath, *Mol. Cells* **2005**, *20*, 1–16.
- [67] C. Davidovich, A. Bashan, T. Auerbach-Nevo, R. D. Yaggie, R. R. Gontarek, A. Yonath, *Proc. Natl. Acad. Sci. USA* **2007**, *104*, 4291–4296.
- [68] J. A. Ippolito, Z. F. Kanyo, D. Wang, F. J. Franceschi, P. B. Moore, T. A. Steitz, E. M. Duffy, *J. Med. Chem.* **2008**, *51*, 3353–3356.
- [69] T. Auerbach, A. Bashan, I. Mermershtain, C. Davidovich, I. Wekselman, E. Zimmerman, H. Rosenberg, A. Mankin, A. Yonath, **2008**; unpublished results.
- [70] L. Lolk, J. Pohlsgaard, A. S. Jepsen, L. H. Hansen, H. Nielsen, S. I. Steffansen, L. Sparving, A. B. Nielsen, B. Vester, P. Nielsen, *J. Med. Chem.* **2008**, *51*, 4957–4967.
- [71] C. Davidovich, A. Bashan, A. Yonath, *Proc. Natl. Acad. Sci. USA* **2008**, in press.
- [72] S. Zaman, M. Fitzpatrick, L. Lindahl, J. Zengel, *Mol. Microbiol.* **2007**, *66*, 1039–1050.
- [73] N. Sonenberg, A. Pause, *Science* **2006**, *314*, 428–429.

---

Received: August 19, 2008